

# Crystallization properties of Ge-Sb and Ge-Bi-Te nanoparticles by pulsed laser irradiation

Takashi MIHARA, Akio TSUCHINO, Shuji SATO, Kazuya HISADA,

Rie KOJIMA, Noboru YAMADA, and Shigeru FURUMIYA

Advanced Technology Research Laboratories, Panasonic Corporation

3-4 Hikaridai, Seika-cho, Soraku-gun, Kyoto 619-0237, Japan

Phone: +81-774-98-2575, FAX: +81-774-98-2406, E-mail: mihara.takashi@jp.panasonic.com

## Abstract

Laser-induced crystallization times ( $\Delta t_c$ ) were investigated for  $\text{Ge}_{10}\text{Sb}_{90}$  and  $\text{Ge}_2\text{Bi}_2\text{Te}_5$  in the forms of nanoparticles less than 50nm in the diameters and 10nm-thick blanket films.  $\Delta t_c$  of nanoparticle samples are longer than that of the blanket film samples. It is remarkable that  $\Delta t_c$  of  $\text{Ge}_{10}\text{Sb}_{90}$  nanoparticles (12 $\mu\text{s}$ ) is 500 times longer than that of the blanket film (24ns), while  $\Delta t_c$  of  $\text{Ge}_2\text{Bi}_2\text{Te}_5$  nanoparticles (80ns) is comparable to that of the blanket film (56ns). This result may have a close relationship with the difference of crystallization process between  $\text{Ge}_{10}\text{Sb}_{90}$  and  $\text{Ge}_2\text{Bi}_2\text{Te}_5$ , which should be taken into account for the optical data storage composed of phase-change nanoparticles.

## 1. Introduction

Nanoparticle phase-change material is one of the promising candidates for the next generation optical data storage. In order to increase the recording density of the phase-change optical memories far beyond the optical resolution limit, it is inherently important suppressing the thermal interference between recording marks. One of the promising methods for that is adoption of isolated nanoparticles. Several studies have been carried out on crystallization properties of nano-sized phase-change materials; e.g., by pulsed electric current in PC-RAM devices<sup>1</sup> or by heating in the inactive gas<sup>2</sup>. However, there are no reports on laser-induced crystallization properties. In this study, we investigated the pulsed laser-induced crystallization times for isolated nanoparticles of  $\text{Ge}_{10}\text{Sb}_{90}$  and  $\text{Ge}_2\text{Bi}_2\text{Te}_5$  by contrast with those for blanket films. It is well-known that  $\text{Ge}_{10}\text{Sb}_{90}$  and  $\text{Ge}_2\text{Bi}_2\text{Te}_5$  are typical high-speed phase-change alloys and show rather different crystallization processes, especially the former is as the “growth-dominant” type<sup>3</sup> and the latter is as the “nucleation-dominant” type<sup>4</sup>.

## 2. Experiments

### 2.1 Preparation of the isolated nanoparticles

Nanoparticles of the two phase-change materials were fabricated by nano-imprint lithography and plasma etching. The upper figure in Fig. 1 shows the preparation procedure. Firstly, the film stack including the 10nm thick phase-change film ( $\text{Ge}_{10}\text{Sb}_{90}$  or  $\text{Ge}_2\text{Bi}_2\text{Te}_5$ ) was formed on the  $\text{SiO}_2$  substrate by sputtering method. Secondly, the UV resin mask pattern of the 50nm-diameter dots at 100nm intervals was imprinted on the top of the film stack. Thirdly,  $\text{CF}_4$  plasma etching of the Si-N film was performed, that was followed by  $\text{O}_2$  ashing process for removing the residual UV resin. Fourthly, Ar etching of the phase-change film was performed. It is expected that the Ar etching will cause less damage to the phase-change material comparing to  $\text{CF}_4$  etching. The AFM images obtained just after the Ar etching are shown at the bottom in Fig. 1. The observed average diameter of  $\text{Ge}_{10}\text{Sb}_{90}$  and  $\text{Ge}_2\text{Bi}_2\text{Te}_5$  particles were 45nm and 47nm, for each. Finally, the obtained nanoparticles were sealed with 15nm-thick Zr-Cr-O protective film. In addition to these nanoparticle samples, blanket film samples having the same stack were prepared as references.

### 2.2 Two lasers optical system

An optical experimental system shown in Fig. 2 was built for evaluating the crystallization times of the samples. A green laser beam ( $\lambda=532\text{nm}$ ) and an infrared laser beam ( $\lambda=785\text{nm}$ ) are coaxially introduced into an objective lens having 0.70-NA and focused onto a sample. The focused spot sizes of the green and the infrared laser beams are 1.0 $\mu\text{m}$  and 1.6  $\mu\text{m}$ , respectively. The pulse duration of the green laser is 50ps (fixed), and the pulse energy level of it can be adjusted to each sample using the transmission-variable ND filter. Both of the pulse duration and the power can be changed for the infrared laser (pulse duration: 2ns~DC). Two sets of an LED changer for illumination and a CCD camera are also equipped for observing the reflection and transmission microscopic images of the sample surfaces. Here, five different wavelengths (white, 448nm, 530nm, 627nm, and 655nm) can be selected for obtaining

a high contrast image just by switching the LEDs.

### 2.3 Evaluation of crystallization times

In order to estimate crystallization times, the minimum pulse duration required for crystallization was studied. Fig. 3 shows the experimental procedure: i) each sample having many nanoparticles on it was uniformly crystallized by DC infrared laser irradiation (initial-state), ii) a center area of the sample was amorphized by the green laser irradiation (write-state), and iii) the area was re-crystallized by the infrared laser irradiation, again (erase-state). This erase process of iii) was achieved at various erase conditions while the write conditions of ii) was fixed to the average pulse energy for amorphization. A sufficiently large optical contrast according to the phase transitions were obtained from the group of approximately 100 nanoparticles, though the change from individual each one nanoparticle was too small for observation. Here, we defined the erase rate of (E) for amorphous nanoparticles as following equation:  $E[\%] = (B_w - B_e) / (B_w - B_i) \times 100$ , where B denotes the grayscale brightness of the microscopic image measured at a laser-irradiated area. The subscripts of *w*, *e*, *i* mean that the state of “write”, “erase”, and “initial”, respectively. Accordingly, the crystallization time of ( $\Delta t_c$ ) is defined as the minimum pulse duration for satisfying  $E > 90\%$  in the process iii).

The above series of experiments were conducted also for the blanket film samples. Thus, the dependence of  $\Delta t_c$  on the compositions and the sample configurations were investigated.

### 3. Results and discussions

The maps in Fig. 4 show the erase rates of  $\text{Ge}_2\text{Bi}_2\text{Te}_5$  and  $\text{Ge}_{10}\text{Sb}_{90}$  samples as a function of pulse duration (horizontal) and the power (vertical) for erasing process. Each lattice point in the maps corresponds to one irradiation condition.

The determined crystallization times ( $\Delta t_c$ ) for each sample were listed in Table 1.  $\Delta t_c$  of the nanoparticle samples become longer than that of the blanket film samples. In the case of  $\text{Ge}_2\text{Bi}_2\text{Te}_5$ ,  $\Delta t_c$  of the nanoparticles (80ns) is comparable to that of the blanket film (56ns). In contrast, in the case of  $\text{Ge}_{10}\text{Sb}_{90}$ ,  $\Delta t_c$  of the nanoparticles (12 $\mu\text{s}$ ) becomes 500 times longer than that of the blanket film (24ns). That is to say,  $\Delta t_c$  of the  $\text{Ge}_{10}\text{Sb}_{90}$  nanoparticles is more than 100 times longer than that of the  $\text{Ge}_2\text{Bi}_2\text{Te}_5$  nanoparticles, while  $\Delta t_c$ s of the blanket films of each material are comparable. It is possible to explain this remarkable difference by the difference of the nucleation processes between the two materials.

Possible re-crystallization models for the amorphous nanoparticles and the amorphous blanket film of each phase-change material are shown in Fig. 5.  $\text{Ge}_2\text{Bi}_2\text{Te}_5$  is known as a nucleation-dominant material, so the isolated  $\text{Ge}_2\text{Bi}_2\text{Te}_5$  nanoparticles can be crystallized as well as the blanket film. On the other hand,  $\text{Ge}_{10}\text{Sb}_{90}$  is known as a growth-dominant material. In the case of the blanket films, crystallization starts at the interface between amorphous and crystalline, which works as the trigger of crystallization. Isolated amorphous  $\text{Ge}_{10}\text{Sb}_{90}$  nanoparticles, however, have no such interfaces at all. The absence of the interface will be a considerable barrier for crystallization.

	Blanket film	Nanoparticles
$\text{Ge}_2\text{Bi}_2\text{Te}_5$	56 ns	80 ns
$\text{Ge}_{10}\text{Sb}_{90}$	24 ns	12 $\mu\text{s}$

Table 1. Determined crystallization times of each material

### 4. Conclusions

We investigated the potential of nanoparticle phase-change alloys for higher density optical data storage. The laser-induced crystallization times ( $\Delta t_c$ ) were examined for nanoparticles of  $\text{Ge}_{10}\text{Sb}_{90}$  and  $\text{Ge}_2\text{Bi}_2\text{Te}_5$  by contrast with those for blanket films.  $\text{Ge}_{10}\text{Sb}_{90}$  nanoparticles around 50nm in the diameters sample showed 500 times longer laser crystallization time ( $\Delta t_c$ ) (12 $\mu\text{s}$ ) compared to that of the blanket film (24ns). This remarkable difference between  $\text{Ge}_{10}\text{Sb}_{90}$  and  $\text{Ge}_2\text{Bi}_2\text{Te}_5$  can be explained by the crystallization processes of these two phase-change alloys: the growth-dominant type for the former, and the nucleation-dominant type for the latter. Thus it can be concluded that nanoparticle phase-change material will be possible and effective; however, it is essentially important to take into account the crystallization mechanisms. In the case of nanoparticle optical media, nucleation-dominant type such as  $\text{Ge}_2\text{Bi}_2\text{Te}_5$  will be favorable than growth-dominant type such as  $\text{Ge}_{10}\text{Sb}_{90}$ .

### References

- [1] J. Lee et al.: IEEE Electron Device Letters, **32**, (2011) 1113.
- [2] Y. Zhang et al.: J. Appl. Phys., **104**, (2008) 074312
- [3] L. van Pieterse et al.: J. Appl. Phys., **97**, (2005) 083520
- [4] J. H. Coombs et al.: J. Appl. Phys. 78, (1995) 4918

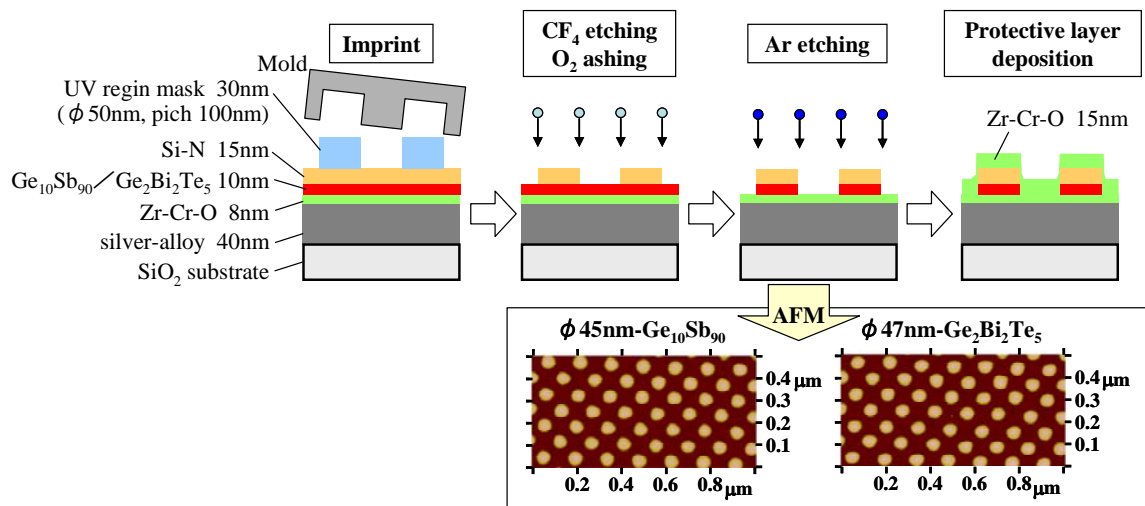


Fig. 1. Preparation procedure of phase-change nanoparticles

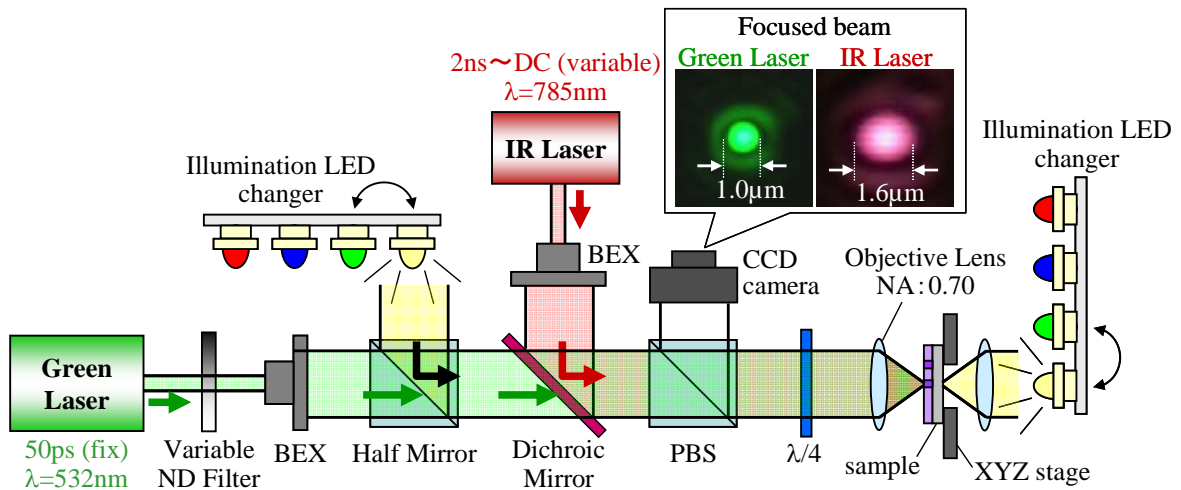


Fig. 2. Two lasers optical system

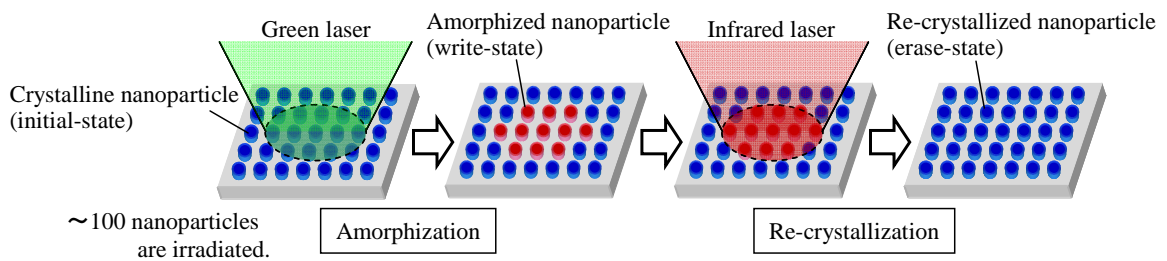


Fig. 3. Experimental procedure for evaluation of the crystallization time

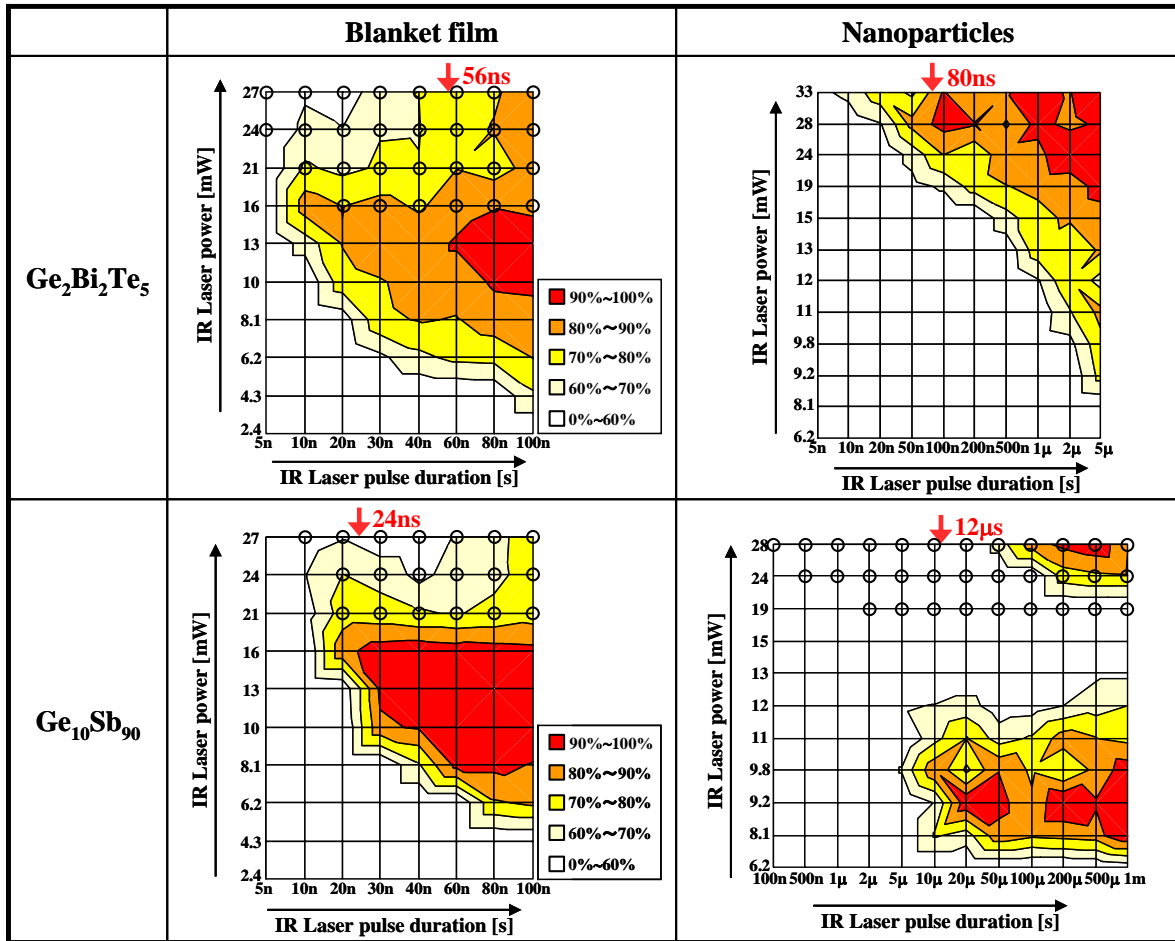


Fig. 4. Erase rates of each sample as a function of pulse duration (horizontal) and the power (vertical) for erasing process. Encircled lattice points mean the conditions in which the phase-change materials can be heated above a melting point. The red arrows indicate determined crystallization times ( $\Delta t_c$ ) for each sample, which corresponds to Table 1.

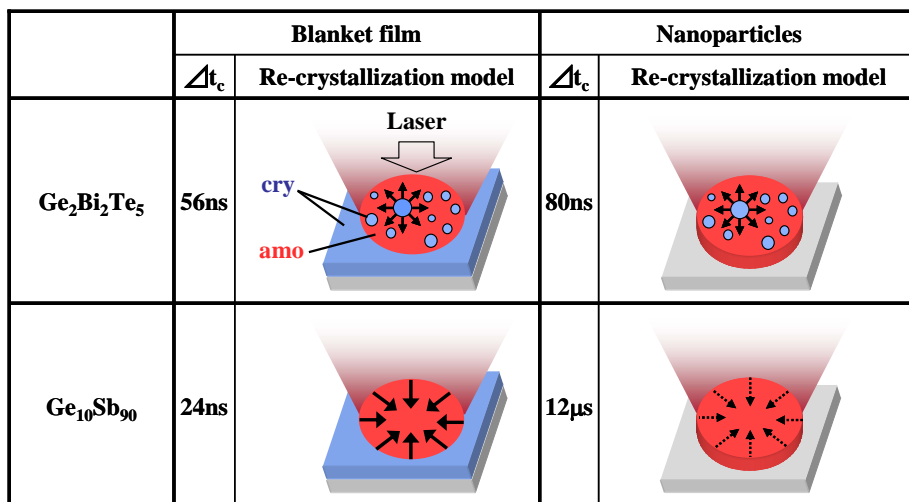


Fig. 5. Possible re-crystallization models of blanket films and nanoparticles of each material